

Supplemental information



Figure S1. Photos and schematics of the experimental setup for *in situ* Mössbauer experiments.

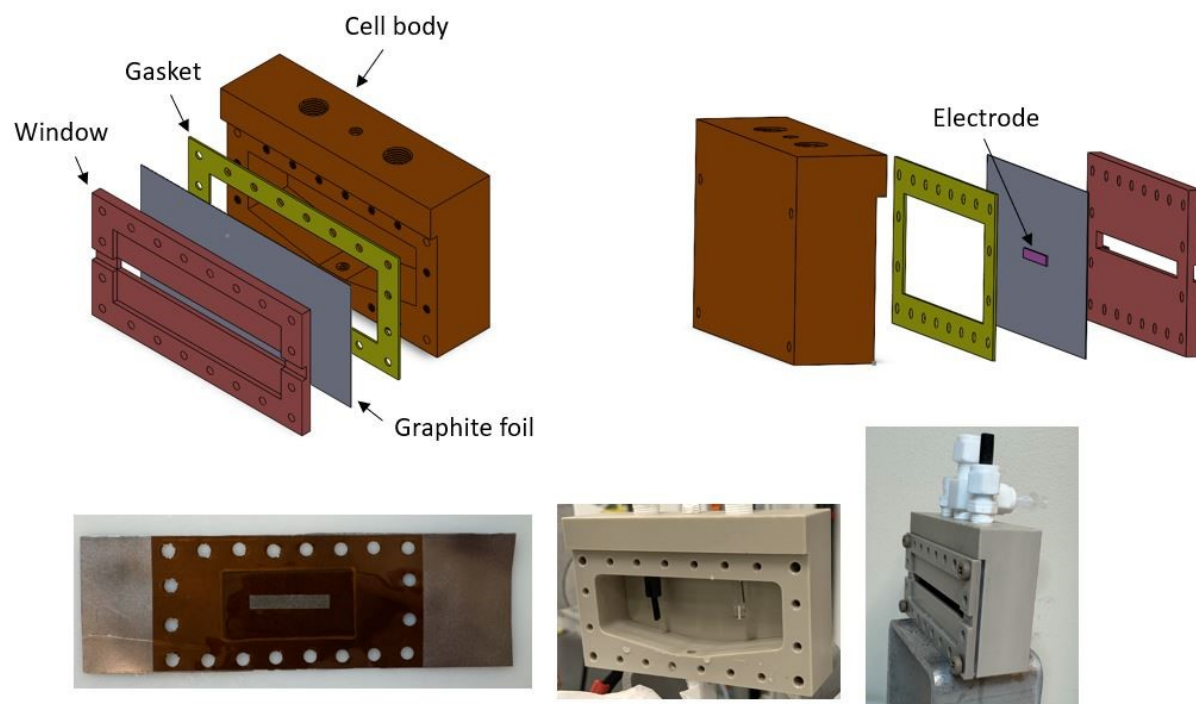


Figure S2. Schematic diagram and experimental photo of the cell assembly for *in situ* XAS experiments.

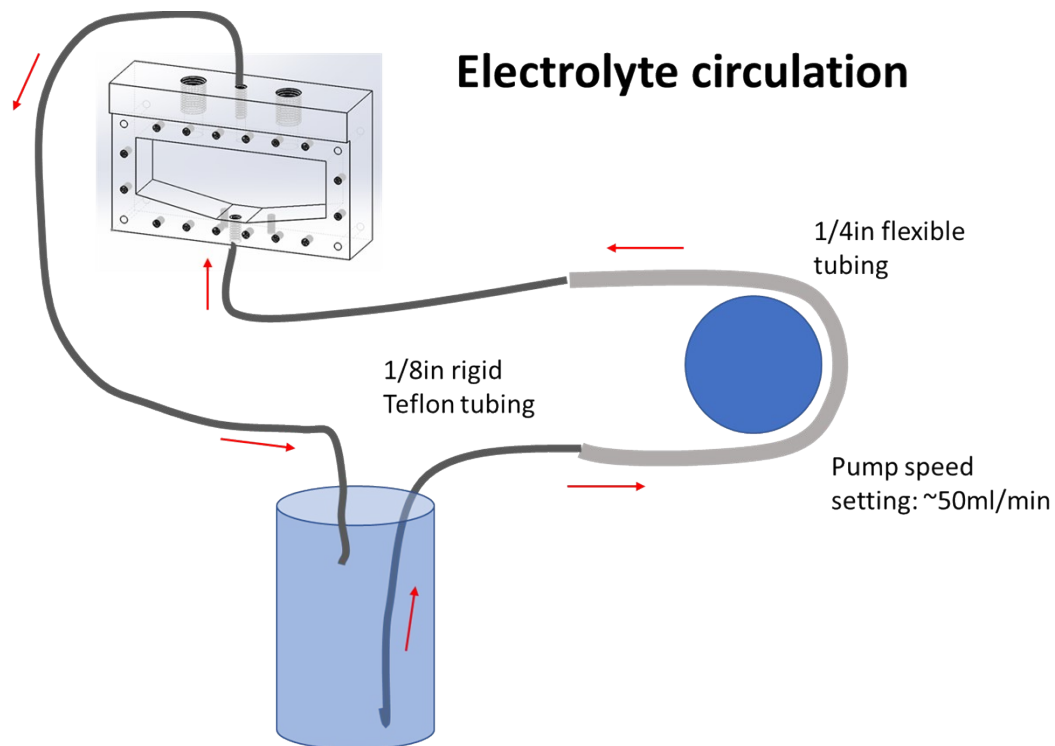


Figure S3. Configuration of electrolyte circulation for *in situ* XAS experiments.

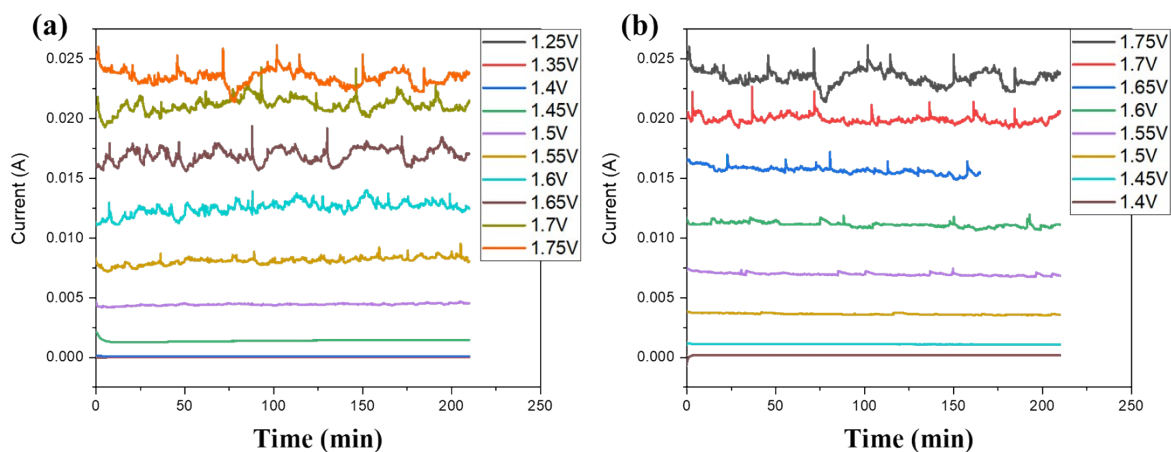


Figure S4. Current-time plots recorded during an *in situ* Mössbauer experiment where (a) shows the potential ramp-up and (b) shows the potential ramp-down. The current response is noisier at potentials higher than 1.55 V likely due to oxygen bubble build up and removal. The noise seemed to be reduced by increasing electrolyte circulation up to 150 mL/min, but the Mössbauer spectrum was broadened due to small vibration of the working electrode (carbon paper). Thus, the flow rate was kept at 50 mL/min to minimize peak broadening.

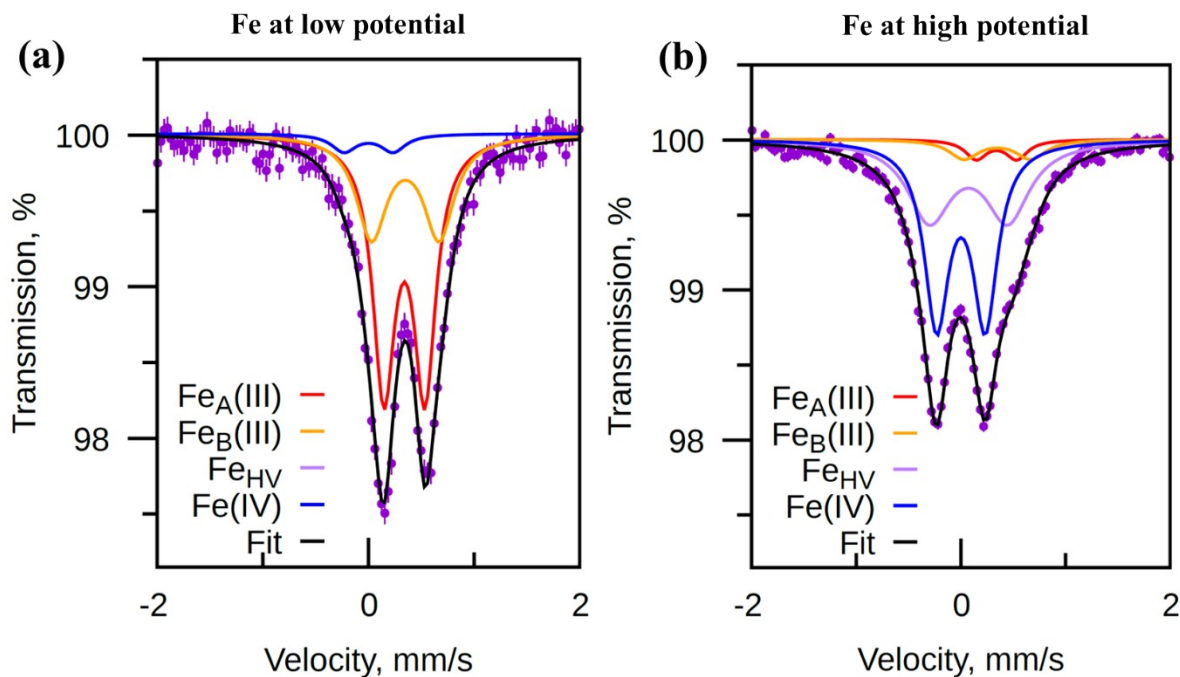


Figure S5. (a) Mössbauer spectrum combining data at low potentials (1.25 V – 1.40 V). (b) Mössbauer spectrum combining data above 1.55 V and back to 1.40 V on the decreasing potential portion of the profile. RFour components are identified and fitted to both spectra.

Table S1 Comparison of experimental conditions and main observations from works of Chen et al.[37], Kuang et al.[38], and this work.

	NiFe hydroxide synthesis	Substrate	BET Surface area	Crystallinity in powder XRD	Fe (IV) % (highest potential)	Fe(IV) IS, QS, (mm/s)	Relaxation
Chen et al. [37]	Co-precipitation and hydrothermal	Carbon paper	Not reported	(003), (006), (012) planes, layered structure	21%, 1.76V (vs. RHE)	IS = -0.25, QS = 0 (singlet)	Fe (IV) remains 20% at 1.49V during cathodic step. No Fe (IV) at OCP.
Kuang et al. [38]	Co-precipitation of NiFe _m -Fe Prussian blue analogues, followed by	Carbon paper	Not reported	XRD pattern comparable with α -Ni(OH) ₂ . Among	40%, 1.57V (vs. RHE)	IS = -0.25, QS = 0 (singlet)	No relaxation observed.

	transformation in alkaline solution.			different Ni/Fe ratios, NiFe _{0.2} shows low crystallinity.			
This work and Osmieri et al., [41].	NiFe aerogel synthesis with supercritical CO ₂ drying, followed by annealing in ambient air at 150°C.	Carbon paper	382 m ² /g	Very low crystallinity with no major peak observable in the XRD pattern.	90%, 1.75V (vs. RHE)	Two doublets: (1) IS = 0.001, QS = 0.465 and (2) IS = 0.07, QS = 0.75.	Fe (IV) content decreases at OCP with half-life ~5 hours. Return to the original state at ~30 hours.

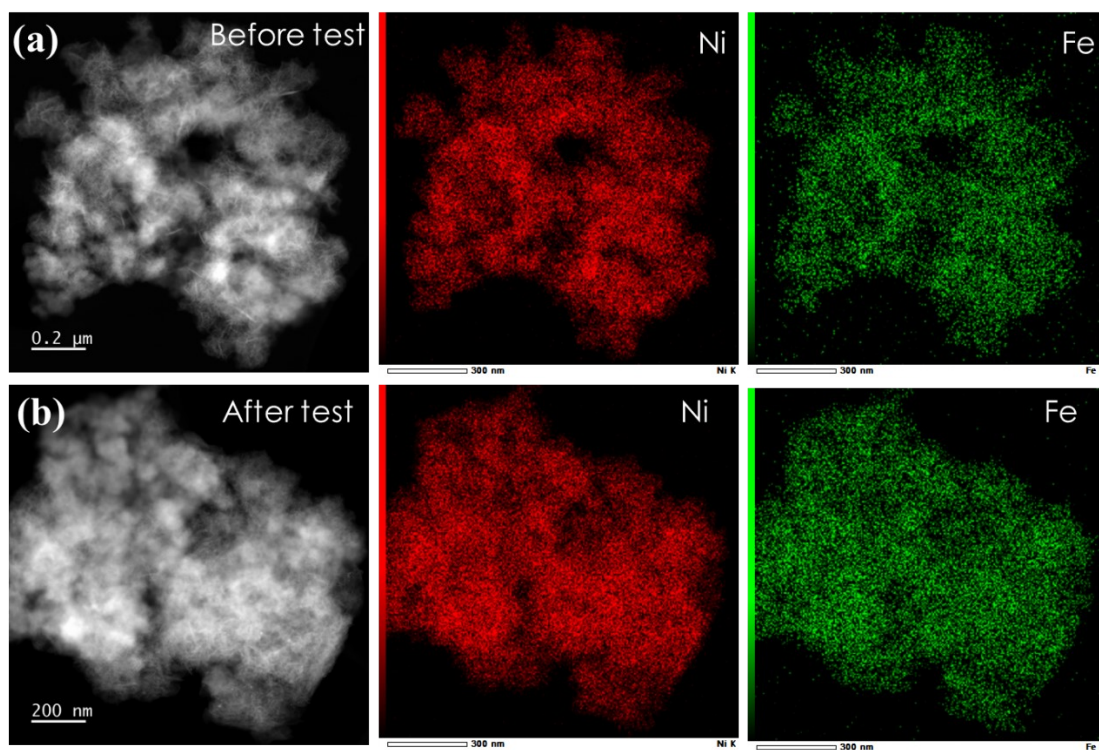


Figure S6. Representative STEM-EDS maps of the Ni₈Fe aerogel catalyst (a) before *in situ* MS test and (b) after *in situ* MS test.

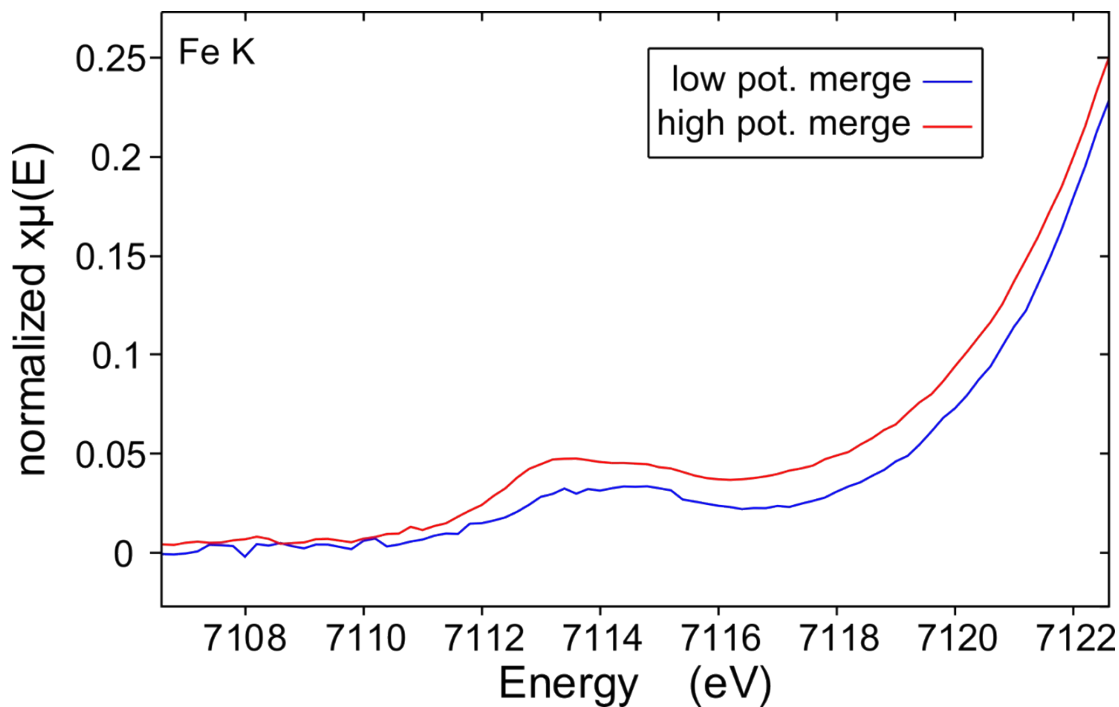


Figure S7. Pre-edge feature at the Fe K-edge increases at potentials where Fe is oxidized, in agreement with literature for the formation of Fe(IV)⁴⁵. Scans at multiple potentials were merged to decrease noise in this feature due to low absorption intensity.

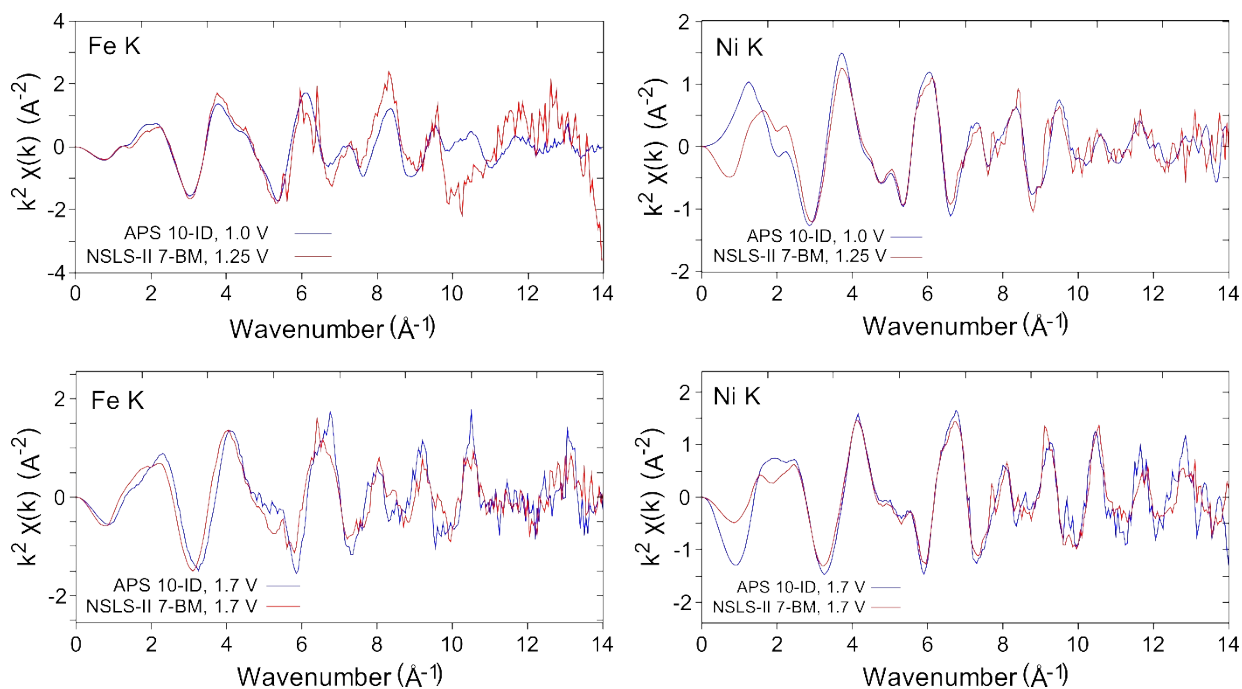


Figure S8. Comparison of EXAFS spectra collected at APS beamline 10-ID and NSLS-II beamline 7-BM at varied potentials. The APS data was used for EXAFS fitting, but the plots demonstrate that the data are consistent across beamlines and that the spectra collected at 1.0 V and 1.25 V are comparable.

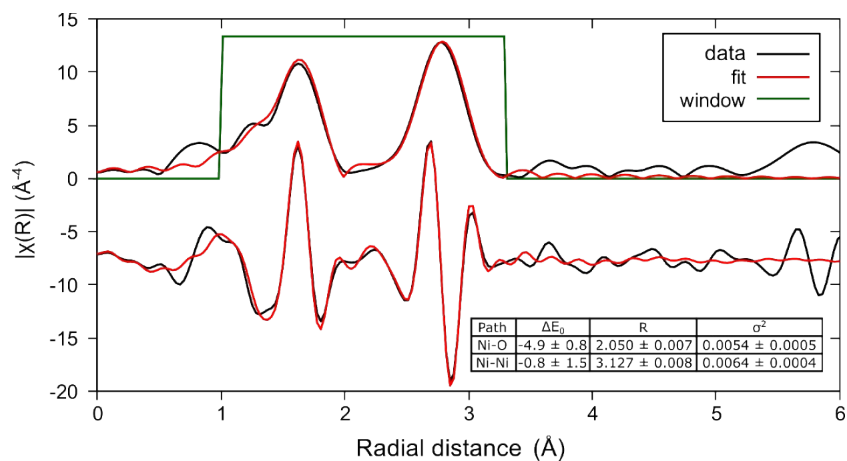


Figure S9. EXAFS fit of the Ni(OH)₂ standard. Coordination numbers / amplitude factors were constrained to known values to determine appropriate Debye-Waller values for sample fits. Separate energy corrections were used for the two paths to allow for adequate fitting of sample fits, and the difference between the two energies (4.2 eV) was used as a standard energy difference. R-factor = 0.0089.

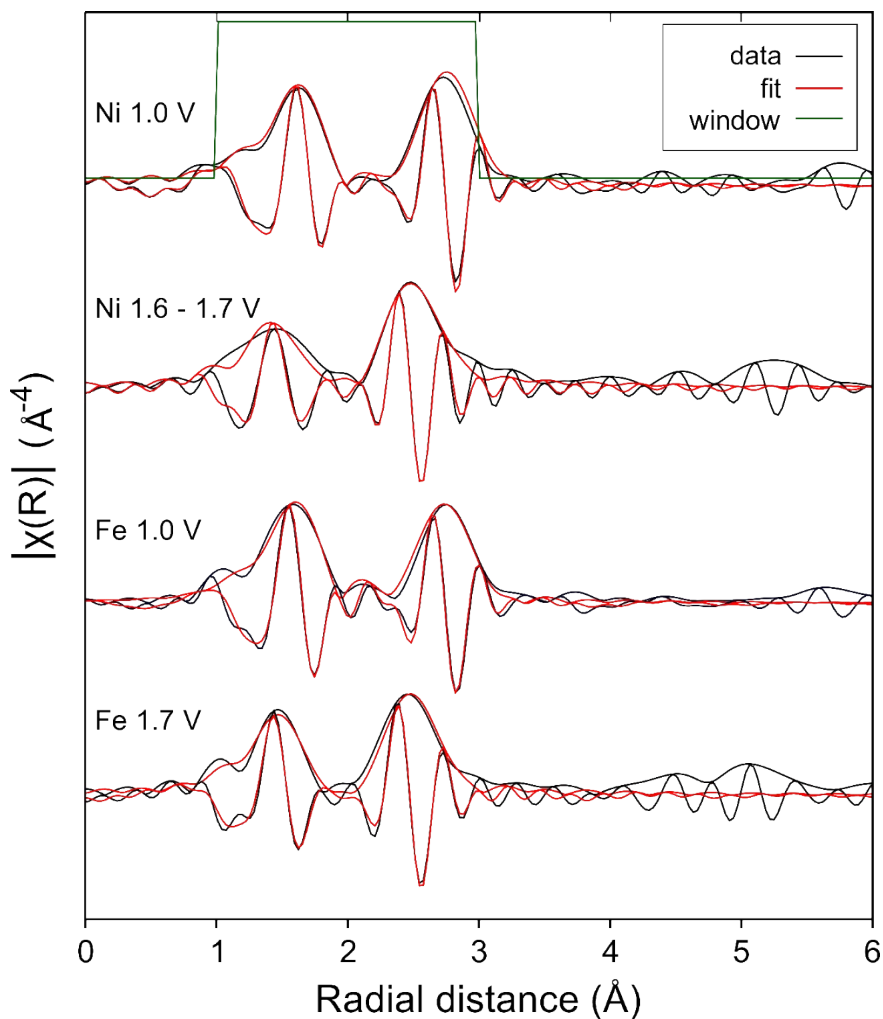


Figure S10. Fit *in situ* EXAFS spectra from Ni K and Fe K-edge measurements at 1.0 and 1.7 V vs. RHE.

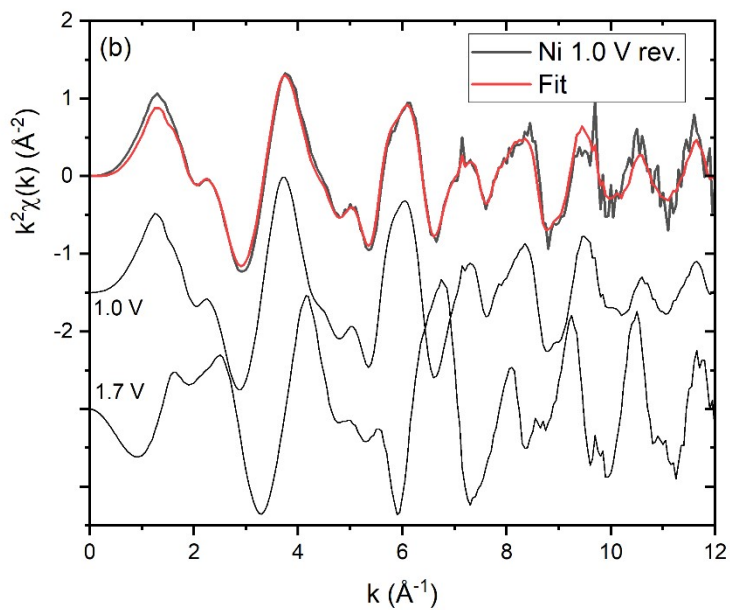
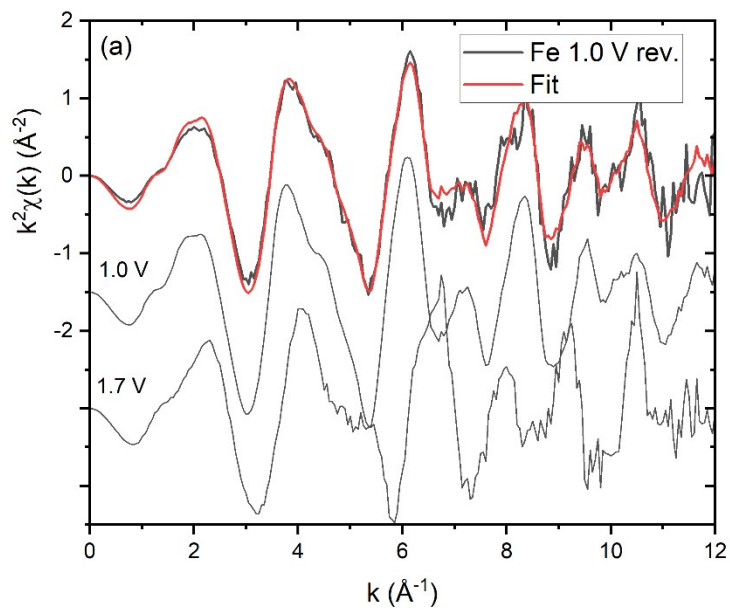


Figure S11. Linear combination fits of (a) Fe and (b) Ni 1.0 V spectra acquired after polarization in the OER potential region (denoted “rev.”) with their respective 1.0 V (initial spectrum, before polarization to 1.7 V) and 1.7 V components (fit range: $k=3.0-11.0 \text{\AA}^{-1}$).

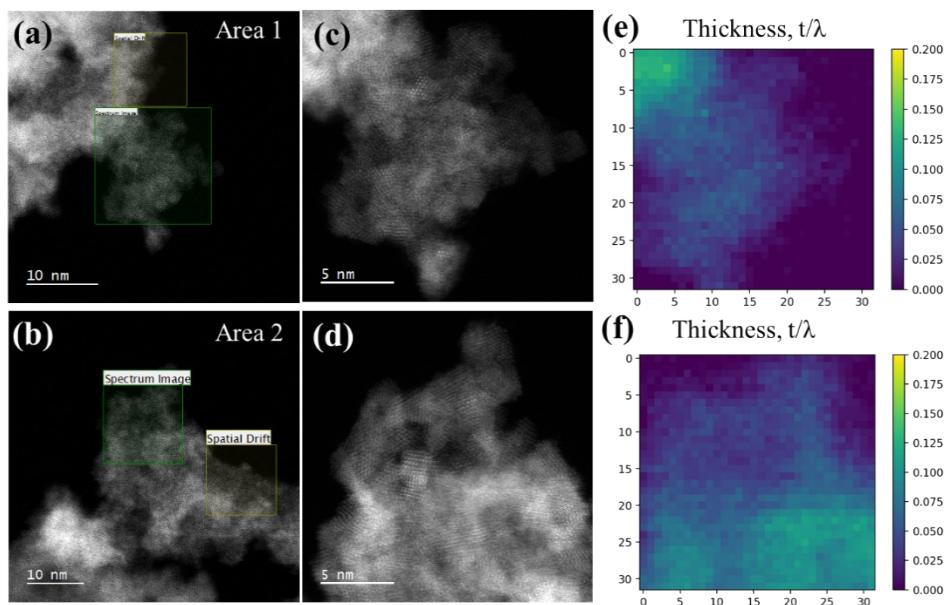


Figure S12. STEM-EELS measurements of the Ni_8Fe aerogel catalyst showing two representative areas (a) and (b) of the nanosheets of NiFe hydroxide at the edge. (c) and (d) are where the spectrum image was acquired. (e) and (f) are the corresponding EELS thickness map in terms of t/λ .

Supplementary note 1: The effect of carbon substrate is negligible for in situ MS and XAS experiments

The substrate used in this work is carbon paper without PTFE treatment. Although carbon materials are generally not stable at OER potentials, carbon paper appears to be much more stable than other types of carbon. The carbon paper used in the current study resulted in no discoloration of the electrolyte after testing and no loss of Fe reflected in MS, which we observed when using other types of carbon paper, particularly those containing microporous layers. Also, the oxidation state and phase of the Ni_8Fe catalyst reverted to the state observed prior to polarization at >1.45 V, indicating that oxidation of carbon, if it occurred, did not affect the conductivity of the carbon and the utilization of the catalyst. In addition, Figure S13 below compares the MS before and after test. The absorption area (in $\% \text{effect} \cdot \text{mm/s}$ unit) is calculated to be 2.29(2) at the start and 2.28(2) after relaxation. Within the error, the absorption area is almost identical which suggests the total mass of Fe is consistent before and after test. This not only demonstrates that the carbon substrate is stable but also the chemical state of Fe is reversible before and after OER. We therefore conclude that over the timeframe of both the MS and XAS measurements, the carbon substrate was stable and had a negligible effect on the experimental results.

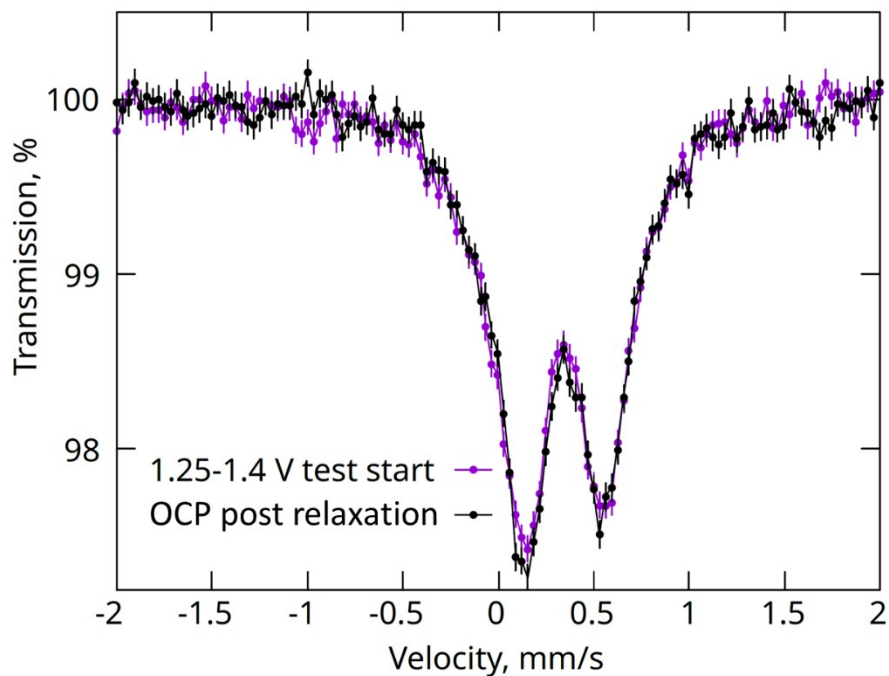


Figure S13. Comparison of the Mössbauer spectra at the start of the test (before Fe(IV) formation) and after the relaxation at OCP. The area (in %effect*mm/s unit) is calculated to be 2.29(2) at the start and 2.28 (2) after relaxation.

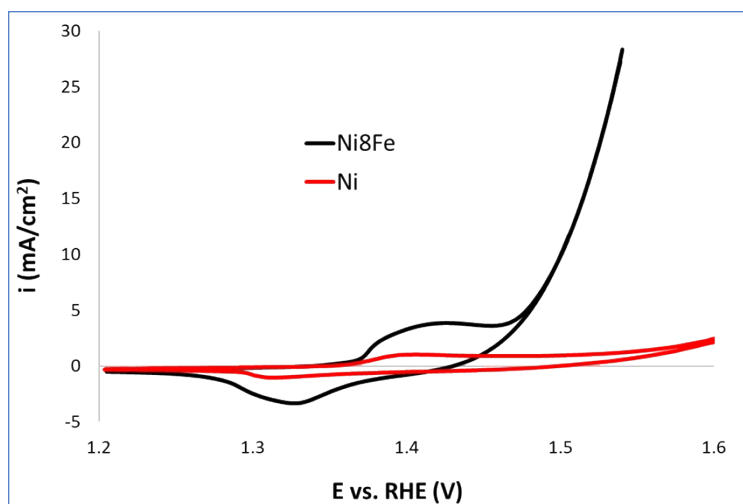


Figure S14. Cyclic voltammograms of Ni₈Fe aerogel catalyst of this study (black) and Ni only catalyst prepared using the same synthesis technique (from Osmieri et al. [41]). The two catalysts have comparable BET surface areas: 425 m² g⁻¹ for Ni only and 382 m² g⁻¹ for Ni₈Fe.